This is a preprint, the final version is subject to change, of the American Mineralogist (MSA)
Cite as Authors (Year) Title. American Mineralogist, in press.
DOI: https://doi.org/10.2138/am-2018-6620

Revision 2

Quantitative analysis of H-species in anisotropic minerals by unpolarized infrared spectroscopy: an experimental evaluation

YANGYANG QIU[1], HAOTIAN JIANG[1], KOVÁCS ISTVÁN[2], QUN-KE XIA[3], AND XIAOZHI YANG[1, *]

[1] State Key Laboratory for Mineral Deposits Research, School of Earth Sciences and Engineering, Nanjing University, Nanjing 210023, PR China

[2] Research Centre for Astronomy and Earth Sciences, Hungarian Academy of Sciences, H-1112 Budapest, Hungary

[3] Institute of Geology and Geophysics, School of Earth Sciences, Zhejiang University, Hangzhou 310027, PR China

*: corresponding author (xzyang@nju.edu.cn)

ABSTRACT

Appreciated attempts have been devoted to use a simple unpolarized infrared analysis on unoriented anisotropic crystals of nominally anhydrous minerals to determine the content of H-species, rather than using the more demanding polarized techniques which determine the true contents of H-species (given that a reliable calibration coefficient is available). In this context, different approaches have been either empirically or theoretically proposed for the quantification; however, the involved accuracy has not been systematically documented

by experimental work of both polarized and unpolarized analyses. In this study, we present a careful evaluation of this issue by conducting experimental measurements on a series of gem-quality OH-bearing olivine, clinopyroxene and orthopyroxene single crystals. The samples were carefully prepared for polarized and unpolarized infrared analyses, and the obtained spectra were used to estimate the H_2O contents. We show that, regardless the applied protocol, a single unpolarized determination is inadequate for quantitative analysis and the uncertainty could be up to ~80%. The unpolarized method of Paterson (1982), by considering the linear absorbance intensity either through a single analysis or by averaging the data from multi-grain analyses, commonly underestimates the H_2O content, by a factor of up to ~6. The other unpolarized calibration method by using the averages of integrated absorbances of unoriented grains is in general of good accuracy, mostly within ±25% even for analyses on 2 grains (with perpendicular indicatrix sections), and the accuracy is even better if as many as 10 gains of random orientations are involved, e.g., within ±10%. Therefore, the latter method may be safely applied to quantify H in anisotropic minerals if a reasonable number of randomly oriented grains are chosen for the analyses. However, the uncertainty is non-systematic, in that it could underestimate but could also overestimate the contents depending on the orientations of the studied unoriented grains. The results lay a solid basis for quantifying H-species in anisotropic minerals and for documenting the quantitative effect of H on the physical properties of the host phases.

Keywords:

OH groups; Quantitative analysis; Unpolarized spectroscopy; Infrared spectroscopy;

This is a preprint, the final version is subject to change, of the American Mineralogist (MSA)
Cite as Authors (Year) Title. American Mineralogist, in press.
DOI: https://doi.org/10.2138/am-2018-6620

INTRODUCTION

The importance of water for the origin and evolution and life on Earth and even the Earth itself makes it an intriguing topic in Earth Sciences. Water in the Earth is rarely present as H_2O molecules (e.g., as seen in the oceans), but is most abundant in the form of hydrogen (H) incorporated in the lattice of various minerals of the planet's interior. In the past decades, H in nominally anhydrous minerals, the dominant constituents of the crust and mantle, has received increasing interest, due to the widespread recognition of the disproportionate importance of even trace amounts of H in governing Earth's geochemical evolution, geophysical properties and geodynamics (Keppler and Smyth 2006; Yang et al. 2014a; Demouchy and Bolfan-Casanova, 2016; Peslier et al., 2017; Xia et al., 2017). In particular, partial melting, element partitioning, ionic diffusion, mechanical strength and electrical conductivity could be affected by small amounts of H in the host minerals (e.g., Inoue 1994; Righter and Drake 1999; Mei and Kohlstedt 2000; Regenauer-Lieb et al. 2001; Hier-Majumder et al. 2005; Huang et al. 2005; Green et al., 2010; Kovács et al., 2012; Yang et al. 2011, 2012; Yang 2012). The effect of H on these aspects, as well as the partitioning, distribution and storage of water inside the Earth, is closely linked to its amount and speciation types, of which the latter is related to the incorporation mechanism. H is structurally present in several forms such as OH groups, molecular H_2O and molecular H_2 (Keppler and Smyth 2006; Yang et al. 2016), and OH groups in nominally anhydrous minerals have attracted particular interest, because the formation involves modification of

67 silicate matrix of the host structure (e.g., by breaking strong Si-O bond and/or creating
68 vacancies). Therefore, the key in many cases is to determine accurately the concentration
69 and species of H.
70
71 Fourier-transform infrared (FTIR) spectroscopy is a very powerful technique, and remains
72 the most widely applied method, for probing H in nominally anhydrous minerals, because
73 of its extreme sensitivity to H, inexpensive costs and non-destructive analyses. Also, it can
74 be easily carried out in situ on very small sample domains, and distinguishes readily
75 different types of H-species such as OH groups, inclusion H_2O, molecular H_2 and organic
76 hydrogen. Moreover, information on the orientations of H in the host structure and on the
77 lengths of hydrogen bond could be deduced if polarized radiation is used, and the exact
78 amount of H can be calculated if an externally determined mineral-specific IR calibration
79 coefficient is available. Accordingly, considerable effort in the past decades has been
80 devoted to develop a simple yet accurate method for measuring the concentration of H in
81 nominally anhydrous minerals with FTIR spectroscopy (e.g., Dowty 1978; Paterson 1982;
82 Libowitzky and Rossman 1996; Asimow et al. 2006; Kovács et al. 2008; Withers 2013;
83 Shuai and Yang 2017). The difficulty involves mainly optically anisotropic minerals and
84 very small grains, where particular attention has been focused on the measurements using
85 polarized or unpolarized analyses. In general, polarized analysis is more demanding than
86 unpolarized work, concerning both sample preparation and FTIR determinations. The
87 general principle of unpolarized FTIR spectroscopy has been theoretically documented,
88 with some key assumptions made in the mathematical deductions (e.g., Kovács et al. 2008;

Sambridge et al. 2008; Withers 2013). Some preliminary studies have been conducted on testing the accuracy of the unpolarized methodology (e.g., Bali et al. 2008; Kovács et al. 2008; Sambridge et al. 2008; Férot and Bolfan-Casanova 2012; Sokol et al. 2013; Withers 2013; Padron-Navarta et al. 2014; Bizimis and Peslier 2015). However, it should be pointed out that the available work has been conducted with only one or just a few samples and/or under the assumption that calculated absorbance with numerical approximations is reliable in reflecting sample true H content. A detailed and comprehensive experimental test of the unpolarized methodology, in particular how accurate the result could be, has not yet been reported.

In this work, we have carried out a detailed experimental evaluation for the quantification of H-species in anisotropic minerals by both polarized and unpolarized FTIR spectrometry. The work is based on a direct comparison between the measured true contents by polarized method and the determined values by unpolarized method, differing from some available studies where the true contents were produced for example by synthesizing the axis-related polarized spectra or by matching the spectra of silicate overtone bands of the samples with those of reported oriented samples (e.g., Bali et al., 2008; Férot and Bolfan-Casanova 2012; Padron-Navarta et al. 2014), and this would make the evaluation more straightforward. The studied samples include a series of gem-quality olivine (Ol), clinopyroxene (Cpx) and orthopyroxene (Opx) single crystals. These crystals, naturally derived and experimentally H-annealed, are characterized by a range of H_2O contents from less than 30 to more than 400 ppm H_2O. We first present a brief technical introduction of the polarized and

unpolarized methods, and then report a careful evaluation of the H quantification by unpolarized analyses.

BACKGROUND

The quantitative measurements of H concentration by FTIR spectroscopy are based on the modified version of the Beer-Lambert law:

$$c = Abs / \varepsilon \cdot t \quad (1)$$

where c is the content of H-species (usually expressed as the equivalent content of H_2O by weight), Abs is the integrated absorbance in the interested region (cm^{-1}, e.g., usually 3700 to 2800 cm^{-1} for OH groups), ε is the calibration coefficient, and t is the thickness of the sample in cm. Therefore, the H content is simply a function of the integrated absorbance normalized to 1 cm thickness (Abs_{total}), given that the calibration coefficient is already known, and Eq (1) becomes

$$c = Abs_{total} / \varepsilon \quad (2)$$

For optically anisotropic minerals, the determined intensity of H-species depends strongly on the orientation of the infrared-active dipole relative to the incident radiation, and Abs_{total} is then the sum of the thickness-normalized integrated absorbance along the three principal axes (X, Y and Z), which are obtained by three polarized FTIR spectra with incident light polarized along the three axes, respectively:

$$Abs_{\text{total}} = Abs_X + Abs_Y + Abs_Z \quad (3)$$

This requires orienting single crystals along some fundamental planes, so that the principal

axes can be determined. However, performing such a procedure on small crystals, either natural or synthetic, is usually hard and time-exhausting, and is sometimes impossible for minerals with low symmetry. To reduce the involved difficulty, Dowty (1978) proposed that Abs_{total} can be produced by polarized analyses along six vibration directions on any three orthogonal planes of a given sample, and subsequently Libowitzky and Rossman (1996) have theoretically and experimentally evaluated this approach.

Empirically, Abs_{total} may be obtained from the thickness-normalized integrated absorbance along any three mutually perpendicular directions (X', Y' and Z'):

$$Abs_{\text{total}} = Abs_{X'} + Abs_{Y'} + Abs_{Z'} \quad (4)$$

Johnson and Rossman (2003) have experimentally tested this approach using one anorthite sample (GRR 1968), and their measured Abs_{total} agreed with that from the three principal axes to within 5% relative. A re-examination of that sample by a later work from the same group (Mosenfelder et al. 2015), however, argued that the method yielded overestimated Abs_{total} by >30%, which may have been caused by heterogeneity of H-species in the sample (Mosenfelder et al. 2015). In a recent report by Shuai and Yang (2017), the validity of Eq (4) has been carefully evaluated with a large number of well-characterized samples and also theoretical approach. The results show that Eq (4) works for samples even at extreme cases, where the absorption bands are both intense (e.g., samples up to ~4 mm thick) and strongly anisotropic, and has the same accuracy as Eq (3) for samples with a reasonable thickness (e.g., up to ~1 mm as what we commonly work with). The method of Eq (4) requires preparing the sample by double-polishing a crystal along any two perpendicular

151 planes only, without the necessarity to orient it. This greatly simplifies the quantification of
152 H-species in anisotropic minerals by polarized FTIR spectroscopy.
153
154 Still, however, there are circumstances where the sample crystals are too small to be
155 prepared for polarized FTIR analyses along different directions. In this case, the frequently
156 adopted alternative is the less demanding unpolarized measurements, which require the
157 preparation of a double-polished section only and are commonly easy to achieve. Two
158 approaches are available here. One is the frequency-dependent calibration of Paterson
159 (1982), which is based on an empirical correlation between the OH stretching frequency
160 and the molar absorption coefficient of quartz and silicate glass:

$$c = \frac{X_i}{150 \cdot \gamma} \int \frac{A(\nu)}{3780 - \nu} d\nu \quad (5)$$

161 where X_i is a density-dependent factor, γ is an orientation factor, and $A(\nu)$ is the
162 thickness-normalized absorbance for a given wavenumber ν (e.g., for a unit thickness of 1
163 cm). This calibration (labeled as Method 1 in this study) was the first generic method
164 specifically designed for determining the concentration of H in minerals and glasses. An
165 apparent merit is that it does not require an externally determined calibration coefficient,
166 and this makes it frequently employed. A critical assumption made for Method 1 is that
167 both the absorption frequency and intensity of a unit amount of H are constants, which are
168 unfortunately not correct for minerals (and glasses). . It should also be pointed out that the
169 γ of 1/3 was proposed by Paterson (1982) under the assumption that the orientation
170 distribution of the OH groups is isotropic (see Table 1 in Paterson 1982), which is certainly

not the case for anisotropic minerals, and that the γ was initially used to relate an unpolarized measurement from a particular direction to Abs_{total}, different from the value of 1/3 proposed in later work which relates the average unpolarized absorbance on unoriented grains to Abs_{total} (Kovács et al. 2008; Withers 2013). The uncertainty of Method 1 was usually assumed to be ~30-50%, although it has been argued that it might be much larger (e.g., Libowitzky and Rossman 1996; Bell et al. 2003). The other approach can be viewed as modified after Eqs (2) and (5), by combining the orientation factor and externally determined calibration coefficients:

$$c = \frac{Abs_{unpol,avg}}{\varepsilon \cdot \gamma} \tag{6}$$

where $Abs_{unpol,avg}$ is the thickness-normalized integrated absorbance averaged over a large number of randomly oriented crystals, and γ is taken as 1/3. This calibration (labeled as Method 2 in this study) has also been widely used (e.g., Katayama and Nakashima 2003; Koga et al. 2003; Xia et al. 2006; Grant et al. 2007; Yang et al. 2008), although the background had not been strictly established. Later, theoretical and empirical work has been carried out, and an equation in the similar form (by replacing γ with 1/3 directly) has been deduced, which explains why a factor 1/3 is required (Kovács et al. 2008; Withers 2013). In principle, Method 2 works for samples where the absorption bands are less intense or weakly anisotropic, e.g., the maximum linear absorbance is <0.3 or the ratio of maximum and minimum absorbance is ~1 (Kovács et al. 2008; Withers 2013). Also, it requires measurements on a statistically meaningful number of randomly oriented grains (e.g., 10 or even more), where caution must be taken for thin sections cut from untreated

191 samples directly since lattice-preferred orientations (LPO) are usually developed in natural
192 and synthetic materials (that is, the sample grains are actually not perfectly unoriented).
193 The uncertainty of Method 2 was usually assumed within ~20-30%. Sometimes, this
194 method has also been applied to samples with only a few grains (e.g., <5) or even for a
195 single grain (e.g., Koga et al. 2003), but the uncertainty has not been evaluated directly.
196

197 ## SAMPLES AND METHODS

198 Samples for the measurements are H-annealed and natural Ol, Cpx and Opx single crystals.
199 The annealed Ol samples are from our previous work (Yang et al. 2014b; Yang 2015, 2016;
200 Shuai and Yang 2017), and the annealed Cpx and Opx samples were from the present work,
201 following the method reported in our previous studies (Yang et al. 2014b; Yang 2015, 2016;
202 Shuai and Yang 2017). A summary of the samples is given in Table 1 and in the Appendix,
203 note that these samples are from three same starting crystals: Ol from Dak Lak (Vietnam),
204 Cpx from Asku (China), and Opx from Tanzania, of which the former two and crystals
205 from the same area as the latter one have been used in our H incorporation experiments
206 (Yang et al. 2014b, 2016; Yang 2015, 2016; Shuai and Yang 2017). In general, the crystals
207 are of gem-quality, although fractures were sometimes developed in the annealed crystals
208 due to stress-related compression and/or decompression during the H-annealing runs at
209 elevated conditions. For each sample, a single crystal was prepared by double-polishing
210 along two perpendicular planes, where polarized FTIR spectra were recorded along three
211 mutually perpendicular directions, following the method of Shuai and Yang (2017), and
212 unpolarized FTIR spectra were taken on the two perpendicular planes. On the other hand,

213 double-polished randomly oriented grains of the natural Cpx and Opx crystals, 10 grains
214 for each, were prepared for unpolarized analyses. Thickness of the prepared samples is
215 usually about 150-900 μm as measured by a Mitutoyo digital micrometer.
216
217 FTIR spectra were obtained with a Bruker Vertex 70V FTIR spectrometer coupled with a
218 Hyperion 2000 microscope at the School of Earth Sciences and Engineering, Nanjing
219 University. A total of 128 or 256 scans were accumulated for each spectrum with a globar
220 source, a KBr/Ge beam-splitter, a mid-band MCT detector, an aperture of ~60×60 μm and
221 a resolution of 4 cm^{-1}. A Zn-Se wire-grid polarizer was used for polarized radiation, and
222 polarized spectra were measured with the electric field vector (*E*) parallel to three mutually
223 perpendicular directions. Optically clean and inclusion- and crack-free areas were chosen
224 for the analyses. During the measurements, the optics of the spectrometer were always kept
225 under vacuum, and the optics of the microscope were continuously purged by purified,
226 H_2O- and CO_2-free air. Baseline corrections of the spectra were carried out by performing
227 a spline fit method defined by points outside the integrated region (Fig. 1). Several baseline
228 corrections were conducted on representative spectra, and the variation of the integrated
229 absorbance of each spectrum, i.e. the arbitrary uncertainty, is usually <10% (mostly <5%).
230 This is normally the best what could be achieved in the community for processing the
231 baseline corrections of any FTIR spectra, either polarized or unpolarized. The integral
232 mineral-specific FTIR absorption coefficients of Bell et al. (1995) for Cpx and Opx and of
233 Bell et al. (2003) for Ol were used for calibrating the H_2O contents. However, adoption of
234 the coefficients does not affect the evaluation of the present study, and in particular, the test

of the accuracy of Method 2 is independent of the choice of coefficient (since the same calibration coefficient is used for both polarized and unpolarized work).

RESULTS AND DISCUSSION

Profile FTIR analyses demonstrate no zoned patterns in the studied crystals (Fig. 2), as also documented in our available reports (Yang et al. 2014b; Yang 2015, 2016). Representative polarized and unpolarized FTIR spectra are shown in Figs. 3 and 4. H_2O contents of the samples are given in Tables 1 and 2, and are plotted in Figs. 5 and 6. A summary of the linear absorbance and H_2O contents of the samples are also given in the Appendix.

H-species in the samples

Significant absorption bands in the wavenumber range 3700-2800 cm^{-1} are observed for all the samples (Figs. 2-4). The bands centered at ~ 3610, 3597, 3573, 3566, 3543, 3524, 3510, 3483, 3448, 3407, 3392, 3353, 3325 and 3179 cm^{-1} for the Ol samples, which are typical for OH groups in many mantle-derived olivines (Matsyuk and Langer 2004; Demouchy et al. 2006) and H-annealed Fe-bearing olivines (Demouchy and Mackwell 2006; Yang and Keppler 2011; Yang 2012, 2015, 2016; Kovács et al. 2012; Yang et al. 2014b; Shuai and Yang 2017; Demouchy et al. 2017). The bands centered at ~3646, 3600, 3558, 3528, 3460 and 3355 cm^{-1} for the Cpx samples and at ~3685, 3600, 3544, 3514, 3415, 3370 and 3065 cm^{-1} for the Opx samples, which are nearly the same as those reported for OH groups in the corresponding minerals, either natural or H-annealed (e.g., Ingrin et al. 1989; Skogby et al. 1990; Rauch and Keppler 2002; Stalder et al. 2015; Turner et al. 2015; Yang et al. 2016;

257 Shuai and Yang 2017; Demouchy et al. 2017).

258

259 It should be noted, however, that the OH bands are actually different between the natural
260 and H-annealed pyroxene samples, although their peak frequencies show some similarity
261 (Figs. 3 and 4). For Cpx, the H-annealed samples demonstrate the most significant band at
262 ~3646 cm^{-1}, with very weak bands at ~3600-3300 cm^{-1}, while the starting natural samples
263 are characterized by intense bands at ~3600-3300 cm^{-1}, with relatively weak band at ~3646
264 cm^{-1} (Figs 3b and 4a). For Opx, the H-annealed samples show the most profound bands at
265 ~3600, 3415 and 3370 cm^{-1}, in obvious contrast to the starting natural samples where the
266 most intense bands are observed at ~3513 and 3063 cm^{-1}; in particular, the sharp band at
267 ~3600 cm^{-1} of the H-annealed samples appears absent in the natural Opx, the sharp band at
268 ~3513 cm^{-1} of the natural Opx is greatly weakened in the H-annealed Opx, and the small
269 band at ~3415 cm^{-1} of the natural Opx is broadened and enhanced in the H-annealed Opx
270 (Figs. 3c and 4b). Similar features have also been reported for Cpx and Opx (Rauch and
271 Keppler 2002; Yang et al. 2016; Shuai and Yang 2017). Because the pyroxenes in this work
272 are from the same starting materials and the chemistry of major- and minor-elements is
273 broadly the same for either the Cpx or Opx samples, the observed differences between the
274 qualitative and quantitative spectral characteristics of natural and H-annealed crystals may
275 reflect different types and populations of defects involved in them. Very likely, the
276 annealings at elevated conditions changed the defect population of the samples, which
277 have in turn affected the incorporation of OH groups (Shuai and Yang, 2017).

278

279 **Quantification of H-species with unpolarized analyses**

280 The H_2O contents of the samples, by polarized analyses along three mutually perpendicular
281 directions of each crystal, are ~25 to 420 ppm H_2O for Ol, 50 to 280 ppm H_2O for Cpx,
282 and 30 to 170 ppm H_2O for Opx (Table 1). The contents of the H-annealed samples
283 reprocessed in this study agree well with those produced in our available work (Yang et al.
284 2014b; Yang 2015, 2016; Shuai and Yang 2017), and the slight difference, commonly
285 within 10% and mostly within 5% relative, is caused by the arbitrary uncertainty involved
286 in the spectral baseline corrections by different operators. These values, representing the
287 true H_2O contents of the samples by considering the "Background" Section above, are used
288 to evaluate the quantification of OH groups with the two frequently adopted unpolarized
289 analyses, namely the Method 1 and Method 2.
290
291 **Method 1**. The H_2O contents estimated by this approach, either obtained on a single grain
292 (or on one of the two planes of each prepared crystal) or the average value of multi-grains
293 (or of the two planes of each prepared crystal), differ clearly from those by polarized
294 analyses (Fig. 3a, 3c and 3e). In general, the content determined by a single unpolarized
295 analysis is apparently lower, and could be underestimated by a factor of up to ~6 for Oli, 3
296 for Cpx and 2 for Opx. The average content of unpolarized analyses on 2 or 10 randomly
297 oriented grains (or planes) demonstrates smaller deviation from the true one, but is still
298 lower by a factor of ~2.5-5.0 (on average 3.2) for Ol, 1.1-2.4 (on average 1.7) for Cpx and
299 1.2-1.4 (on average 1.3) for Opx (according to the data in Table 1). Broadly speaking, this
300 method works better for Cpx and Opx than for Ol, and clearly a general upward revision is

needed for the estimated H_2O content. The observation that the H_2O content of Ol calibrated by this method is ~3 times lower is in excellent agreement with that of Bell et al. (2003), where the same conclusion has been reached for H_2O in natural olivines. This would mean that the method is actually inadequate for precise OH quantification. In case very rough information of sample H_2O content is required only or an externally determined calibration coefficient is not available for the target mineral, this method could be applied; however, the uncertainty could be up to ~80%, even when the average value of analyses on multi-grains is considered.

Method 2. The H_2O contents estimated by this approach, either obtained on a single grain (or on one of the two planes of each prepared crystal) or the average value of multi-grains (or of the two planes of each prepared crystal), also show a variable but generally low degree of deviation from those determined by polarized measurements (Fig. 3b, 3d and 3f). In general, the value by a single unpolarized analysis ranges from ~40% lower to 70% higher than the true content for all the studied samples and minerals, although the data mostly cluster around the 1:1 reference line. The average contents of unpolarized analyses on 2 or 10 randomly oriented grains (or planes) fall mostly within ±25% of the true ones, although the deviation can in some cases be ~40%. Therefore, the H_2O content in optically anisotropic minerals estimated by Method 2 is generally more accurate that that by Method 1. The accuracy of a single unpolarized analysis is relatively poor, as argued theoretically (Kovács et al. 2008; Withers 2013). The average contents from two unpolarized analyses on two different planes of the samples, in other words two grains of different orientations,

323 are usually acceptable given an accuracy level of ±25%. However, it does not mean that
324 unpolarized measurements on two randomly-chosen unoriented grains of a given sample
325 could always yield a similar accuracy in H_2Ocontent, because the two planes in this study
326 are not arbitrary but mutually perpendicular (meaning that the orientations of the OH
327 vectors are spatially relevant) which could affect the measured spectra and thus the H_2O
328 content. This is actually obvious from our measured data on the natural cpx and opx, where
329 the content of a single unpolarized analysis could be ~60% higher or 40% lower than the
330 true value (Fig. 5d and 5f) and the average of two analyses on two grains could deviate by
331 ~40-60% in the extreme cases. For both the natural cpx and opx samples, the average H_2O
332 contents from unpolarized analyses on 10 unoriented grains of random orientations are
333 essentially the same as those determined by polarized measurements, consistent with each
334 other within ~7% (Fig. 5 and Table 2).
335
336 In summary, Method 2 has apparent advantage over Method 1 in the context of accuracy in
337 the quantification, as the uncertainty could be ~25% or smaller even only two unpolarized
338 measurements from two unoriented grains are considered. For a given sample, the relative
339 variation of H_2O contents estimated by a single unpolarized analysis is usually larger for
340 cpx and opx than for oli (demonstrated by both Method 1 and Method 2: Fig. 5), which
341 could be reasonably accounted for by the more anisotropic absorption bands in the former
342 than in the latter (Figs. 3 and 4 and Appendix). However, it appears clear that the average
343 value produced by Method 2 is acceptable mostly with an accuracy within ±25% (Fig. 5d
344 and 5f), even for samples whose absorption bands are both strong and strongly anisotropic

(Figs. 3 and 4 and Appendix). A regression processing of all the data demonstrates that the average contents by Method 2 are globally in excellent agreement with the true values by polarized work (Fig. 6). Thus, it would be usually fine to apply Method 2 to both natural and synthetic samples where the information of H_2O contents is to be determined. In some studies, a particularly high level of accuracy is required for quantifying the H content, e.g., for documenting the quantitative effect of OH on some physical properties of the host minerals such as ionic diffusivity and electrical conductivity. Concerning these studies, the application of Method 2 may yield H_2O contents of acceptable accuracy (within ±25% even only from two unpolarized measurements on two unoriented grains), but it may cause large uncertainty to H-related physical parameters because the uncertainty is non-systematic, in that it could underestimate but could also overestimate the contents (Figs. 5 and 6). For example, electrical conductivity is sensitive to OH in nominally anhydrous minerals, and the large variation of the experimentally determined OH-related exponential factor, *r* in the Arrhenius equation which is linked to the nature of the charged H and ranges from ~0.6 to 1.5 in available reports (e.g., Huang et al. 2005; Yang et al. 2011, 2012; Yang 2012; and references therein), is very likely caused by the non-systematic error in characterizing the H_2O contents of the involved samples (Yang et al. 2012; Li et al., 2017).

Finally, the experimental test demonstrates that Method 2 works even for samples whose bands are both intense and strongly anisotropic (Fig. 5 and Appendix). This, in fact, differs from the theory in available reports that the method works in principle for samples with

either less anisotropic bands or the maximum linear intensity is relatively small (i.e. <0.3: Kovács et al. 2008; Withers 2013). In particular, Withers (2013) has shown by numerical simulation that, for unpolarized measurements on randomly oriented grains with a number of up to 10, the yielded average values always underestimate the H_2O content, although the convergence toward the true content is apparent with increasing the number of studied grains (see Fig. 5 in that paper). This is not supported by our experimental work where the average values of unpolarized analyses on randomly oriented grains, 2-10 for each sample, could either overestimate or underestimate the contents (i.e. non-systematic patterns: Fig. 5b, 5d and 5f). The difference might be caused by some assumptions or approximations made in the theoretical deductions of previous work, concerning for example the complex relationship between spectral absorbance and transmittance and the simplification in the mathematical processing including the numerical integration of some complex equations (see more details in: Kovács et al. 2008; Withers 2013). This means that the requirements for applying Method 2 is actually not that strict as those established theoretically (Kovács et al. 2008; Withers 2013), and the data of this work may provide a basis for reevaluating the theoretical background in early work. Further studies on the theoretical background of Kovács et al. (2008) and Withers (2013) would reconcile the difference between theoretical and experimental approaches.

IMPLICATIONS

By carrying out a careful experimental work on a series of H-bearing Ol, Cpx and Opx with both polarized and unpolarized measurements, the results of this study provide by far

the first systematic evaluation for quantifying H-species in anisotropic minerals by unpolarized infrared spectroscopy. Our data demonstrate clearly that the H_2O content estimated by a single unpolarized analysis could be inaccurate if the polarized absorbance indicatrix is highly anisotropic, and the uncertainty could be up to ~80% in extreme cases. Moreover, unpolarized Method 1 commonly underestimate the H_2O content by a factor of up to ~6, even when the average of multi-grain measurements is taken into account, and unpolarized Method 2 is in general more precise, with an accuracy mostly within ±25%. Method 1 could be employed to estimate the H_2O content of samples when externally determined mineral-specific calibration coefficients are not available, but the very large uncertainty must be considered. Method 2 could be applied safely to samples where only rough information is required for the amount of H-species, but particular caution must be paid to the random orientation of the involved grains because of the development of LPO in natural and synthesized samples. For example, unpolarized analyses on 10-20 or even more unoriented grains in a rock section with strong LPO of the studied mineral may be physically equivalent to work on only one or just a few grains.

Accepting the uncertainties, unpolarized FTIR determinations could be used to quantify the amount of H in optically anisotropic minerals. This can be readily conducted, because the required procedure of sample preparation is pretty simple (when compared to polarized work). Our results provide a solid basis for evaluating the accuracy of the yielded data and for future studies on measuring H_2O contents in anisotropic minerals and on a quantitative understanding of the effect of water on physical properties of the host minerals. In case the

411 mineral grains in a sample section are randomly oriented, analyses of 10 grains by Method
412 2 could yield H_2O contents of nearly the same accuracy as the polarized measurements, but
413 the prerequisite might not be easily reached for simply-prepared sample sections (e.g., the
414 grains are not perfectly randomly oriented). It should be further noted that the protocols for
415 calculating water contents are actually different between Method 1 and Method 2 (See the
416 Background Section). Therefore, the contents of H-species estimated by Method 1 can only
417 be recalculated to Method 2 if the original spectra are provided, and a simple conversion of
418 the concentrations by a simple factor would introduce large non-systematic uncertainty. At
419 last, we would like to emphasize that, for very precise work, polarized FTIR analyses
420 along the three principal axes (the standard approach) or along any three random but
421 orthogonal directions (the modified method: Shuai and Yang (2017)) should be considered
422 first if the samples allow the preparation (e.g., with a suitable grain size).
423

424 **ACKNOWLEDGEMENTS**

425 Q.Y. thanks Hanyong Liu and Hongzhan Fei for assistance with sample preparation, FTIR
426 analyses and data processing. We thank the constructive comments by George Rossman
427 and one anonymous reviewer and the editorial handling by Melinda Dyar. This study was
428 supported by grants to X.Y. from the National Basic Research Program of China
429 (2014CB845904), the National Science Foundation of China (41590622, 41725008 and
430 41372041), and the Fundamental Research Funds for the Central Universities (P.R. China),
431 and partly by grant to I.K. from the funding scheme of the National Innovation, Research
432 and Developments Office (Hungary, K128122).

REFERENCES CITED

Asimow, P.D., Stein, L.C., Mosenfelder, J.L., and Rossman, G.R. (2006) Quantitative polarized infrared analysis of trace OH in populations of randomly oriented mineral grains. American Mineralogist, 91, 278–284.

Bali, E., Bolfan-Casanova, N., and Koga, K. T. (2008) Pressure and temperature dependence of h solubility in forsterite: an implication to water activity in the earth interior. Earth and Planetary Science Letters, 268, 354-363.

Bell, D.R., Ihinger, P.D., and Rossman, G.R. (1995) Quantitative analysis of trace OH in garnet and pyroxenes. American Mineralogist, 80, 465–474.

Bell, D.R., Rossman, G.R., Maldener, J., Endisch, D., and Rauch, F. (2003) Hydroxide in olivine: a quantitative determination of the absolute amount and calibration of the IR spectrum. Journal of Geophysical Research: Solid Earth, 108, B2, 2105, doi: 10.1029/2001JB000679.

Bizimis, M., and Peslier, A. H. (2015) Water in hawaiian garnet pyroxenites: implications for water heterogeneity in the mantle. Chemical Geology, 397, 61-75.

Demouchy, S., and Mackwell, S. (2006) Mechanisms of hydrogen incorporation and diffusion in iron-bearing olivine. Physics and Chemistry of Minerals, 33, 347–355.

Dowty, E. (1978) Absorption optics of low-symmetry crystals-application to titanian clinopyroxene spectra. Physics and Chemistry of Minerals, 3, 173-181.

Férot, A., and Bolfan-Casanova, N. (2012) Water storage capacity in olivine and pyroxene to 14 GPa: implications for the water content of the earth's upper mantle and nature of seismic discontinuities. Earth and Planetary Science Letters, 349-350, 218-230.

Grant, K.J., Ingrin, J., Lorand, J.P., and Dumas, P. (2007) Water partitioning between mantle minerals from peridotite xenoliths. Contributions to Mineralogy and Petrology, 154, 15-34.

Hier-Majumder, S., Mei, S., and Kohlstedt, D. L. (2005) Water weakening of clinopyroxene in diffusion creep. Journal of Geophysical Research Atmospheres, 110, doi: 10.1029/2004JB003414.

Huang, X., Xu, Y., and Karato, S.I. (2005) Water content in the transition zone from electrical conductivity of wadsleyite and ringwoodite. Nature, 434, 746-749.

Ingrin, J., Latrous, K., Doukhan, J. C., and Doukhan, N. (1989) Water in diopside: an electron microscopy and infrared spectroscopy study. European Journal of Mineralogy, 1, 327-341.

Inoue, T. (1994) Effect of water on melting phase relations and melt composition in the Mg_2SiO_4-$MgSiO_3$-H_2O system up to 15 GPa. Physics of the Earth and Planetary Interiors, 85, 237-263.

Johnson, E.A., and Rossman, G.R. (2003) The concentration and speciation of hydrogen in feldspars using FTIR and ^1H MAS NMR spectroscopy. American Mineralogist, 88, 901-911.

Katayama, I., and Nakashima, S. (2003) Hydroxyl in clinopyroxene from the deep subducted crust: evidence for H_2O transport into the mantle. American Mineralogist, 88, 229-234.

Keppler, H., and Smyth, J.R. (2006) Water in nominally anhydrous minerals. Mineralogical Society of America, Washington, pp. 478.

Koga, K., Hauri, E., Hirschmann, M., and Bell, D. (2003) Hydrogen concentration analyses using SIMS and FTIR: Comparison and calibration for nominally anhydrous minerals. Geochemistry Geophysics Geosystems, 4, 1019, doi: 10.1029/2002GC000378.

Kovács, I., Hermann, J., O'Neill, H. S. C., Gerald, J. F., Sambridge, M., and Horvath, G. (2008) Quantitative

absorbance spectroscopy with unpolarized light: Part II. Experimental evaluation and development of a protocol for quantitative analysis of mineral IR spectra. American Mineralogist, 93, 765–778.

Libowitzky, E., and Rossman, G.R. (1996) Principles of quantitative absorbance measurements in anisotropic crystals. Physics and Chemistry of Minerals, 23, 319–327.

Matsyuk, S.S., and Langer, K. (2004) Hydroxyl in olivines from mantle xenoliths in kimberlites of the Siberian platform. Contributions to Mineralogy and Petrology, 147, 413–437.

Mei, S., and Kohlstedt, D.L. (2000) Influence of water on plastic deformation of olivine aggregates: 2. Dislocation creep regime. Journal of Geophysical Research: Solid Earth, 105, 21471–21481.

Mosenfelder, J.L., Rossman, G.R., and Johnson, E.A. (2015) Hydrous species in feldspars: a reassessment based on FTIR and SIMS. American Mineralogist, 100, 1209-1221.

Padrón-Navarta, J. A., Hermann, J., and O'Neill, H. S. C. (2014) Site-specific hydrogen diffusion rates in forsterite. Earth and Planetary Science Letters, 392(392), 100-112.

Paterson, M. (1982) The determination of hydroxyl by infrared absorption in quartz, silicate glasses and similar materials. Bulletin de Mineralogie, 105, 20-29.

Rauch, M., and Keppler, H. (2002) Water solubility in orthopyroxene. Contributions to Mineralogy and Petrology, 143, 525–536.

Regenauer-Lieb, K., Yuen, D.A., and Branlund, J. (2001) The initiation of subduction: criticality by addition of water? Science, 294, 578–580.

Righter, K., and Drake, M. J. (1999) Effect of water on metal-silicate partitioning of siderophile elements: a high pressure and temperature terrestrial magma ocean and core formation. Earth and Planetary Science Letters, 171, 383-399.

Sambridge, M., Gerald, J. F., Kovács, I., O'Neill, H. S. C., and Hermann, J. (2008) Quantitative absorbance spectroscopy with unpolarized light: part I. physical and mathematical development. American Mineralogist, 93, 751-764.

Shuai, K., and Yang, X. (2017) Quantitative analysis of H-species in anisotropic minerals by polarized infrared spectroscopy along three orthogonal directions. Contributions to Mineralogy and Petrology, 172, 14, doi: 10.1007/s00410-017-1336-2.

Skogby, H, Bell, D.R., and Rossman, G.R. (1990) Hydroxide in pyroxene: variations in the natural environment. American Mineralogist, 75, 764–774.

Sokol, A. G., Kupriyanov, I. N., and Palyanov, Y. N. (2013) Partitioning of H_2O between olivine and carbonate–silicate melts at 6.3 Gpa and 1400 °C: implications for kimberlite formation. Earth and Planetary Sciences Letters, 383, 58-67.

Stalder, R., Karimova, A., and Konzett, J. (2015) OH-defects in multiple-doped orthoenstatite at 4-8 GPa: filling the gap between pure and natural systems. Contributions to Mineralogy and Petrology, 169, 38, doi: 10.1007/s00410-015-1133-8.

Turner, M., Ireland, T., Hermann, J., Holden, P., Padrón-Navarta, J. A., Hauri, E.H., Turner, S. (2015) Sensitive high resolution ion microprobe-stable isotope (SHRIMP-SI) analysis of water in silicate glasses and nominally anhydrous reference minerals. Journal of Analytical Atomic Spectrometry, 30, 1706-1722.

Withers, A. C. (2013) On the use of unpolarized infrared spectroscopy for quantitative analysis of absorbing species in birefringent crystals. American Mineralogist, 98, 689–697.

Xia, Q.K., Yang, X.Z., Deloule, E., Sheng, Y.M., and Hao, Y.T. (2006) Water in the lower crustal granulite xenoliths from Nushan, eastern China. Journal of Geophysical Research: Solid Earth, 111, doi: 10.1029/2006JB004296.

Yang, X.Z., Xia, Q.K., Deloule, E., Dallai, L., Fan, Q.C., and Feng, M. (2008) Water in minerals of

519 continental lithospheric mantle and overlying lower crust: a comparative study of peridotite and granulite
520 xenoliths from the North China Craton. Chemical Geology, 256, 33-45.
521 Yang, X., and Keppler, H. (2011) In-situ infrared spectra of OH in olivine to 1100 ^{o}C. American Mineralogist,
522 96, 451–454.
523 Yang, X., Keppler, H., McCammon, C., Ni, H., Xia, Q., and Fan, Q. (2011) The effect of water on the
524 electrical conductivity of lower crustal clinopyroxene. Journal of Geophysical Research: Solid Earth, 116,
525 B04208, doi: 10.1029/2010JB008010
526 Yang, X. (2012a) Orientation-related electrical conductivity of hydrous olivine, clinopyroxene and
527 plagioclase and implications for the structure of the lower continental crust and uppermost mantle. Earth
528 and Planetary Science Letters, 317–318, 241–250.
529 Yang, X. (2012b) An experimental study of H solubility in feldspars: effect of composition, oxygen fugacity,
530 temperature and pressure and implications for crustal processes. Geochimica et Cosmochimica Acta, 97,
531 46–57.
532 Yang, X., Keppler, H., McCammon, C., and Ni, H. (2012) Electrical conductivity of orthopyroxene and
533 plagioclase in the lower crust. Contributions to Mineralogy and Petrology, 163, 33-48.
534 Yang, X., Keppler, H., Dubrovinsky, L., and Kurnosov, A. (2014a) In-situ infrared spectra of hydroxyl in
535 wadsleyite and ringwoodite at high pressure and high temperature. American Mineralogist, 99, 724–729.
536 Yang, X., Liu, D., and Xia, Q. (2014b) CO_2-induced small water solubility in olivine and implications for
537 properties of the shallow mantle. Earth and Planetary Science Letters, 403, 37–47.
538 Yang, X. (2015) OH solubility in olivine in the peridotite-COH system under reducing conditions and
539 implications for water storage and hydrous melting in the reducing upper mantle. Earth and Planetary
540 Science Letters, 432, 199–209.
541 Yang, X. (2016) Effect of oxygen fugacity on OH dissolution in olivine under peridotite-saturated conditions:
542 an experimental study at 1.5–7 GPa and 1100–1300 °C. Geochimica et Cosmochimica Acta, 173, 319–
543 336.
544 Yang, X., Keppler, H., and Li, Y. (2016) Molecular hydrogen in mantle minerals. Geochemical Perspectives
545 Letters, 2, 160-168.

546

FIGURE CAPTIONS

Fig. 1 Representative spectra of olivine (a), clinopyroxene (b) and orthopyroxene (c) for baseline correction. Uncorrected, baseline and corrected spectra are shown from top to bottom by black, blue and red lines, respectively. The spectra were normalized to 1 cm thickness and vertically offset.

Fig. 2 Representative profile FTIR spectra of H-species in olivine (a), clinopyroxene (b) and orthopyroxene (c). Numbers above each spectrum show the integrated absorbance (cm^{-2}, with an uncertainty of <10%, mostly <5%, due to baseline correction) and the estimated distance from crystal center (μm in parentheses). The spectra were normalized to 1 cm thickness and vertically offset.

Fig. 3 Representative polarized and unpolarized FTIR spectra of H-species in H-annealed olivine (a), clinopyroxene (b) and orthopyroxene (c). The bottom polarized spectra were taken along three random but orthogonal directions, and the top unpolarized spectra were taken over two perpendicular planes. Conditions for the H-annealing of the samples are shown in the figures. The spectra were normalized to 1 cm thickness and vertically offset.

Fig. 4 Polarized and unpolarized FTIR spectra of H-species in natural clinopyroxene (a) and orthopyroxene (b). The bottom polarized spectra were taken along three random but orthogonal directions, and the top unpolarized spectra were taken on 10 randomly oriented grains. The spectra were normalized to 1 cm thickness and vertically offset.

Fig. 5 Plots of H_2O contents determined by polarized measurements and by unpolarized

Method 1 (a) and unpolarized Method 2 (b). Data points were taken from Tables 1 and 2. Open symbol represents a single unpolarized analysis, and solid symbol represents the average value of multi-grain analyses (purple, by averaging 2 unpolarized spectra from 2 perpendicular planes of a crystal; red, by averaging 10 unpolarized spectra from 10 randomly oriented grains). Dashed lines are for reference only. Error bars were assumed 10% relative (note that the uncertainty of our data was usually <10% and mostly <5% relative: see text)

Fig. 6 Plot of H_2O contents by polarized analyses and by unpolarized Method 2. The average contents of Tables 1 and 2, shown also in Fig. 5, are plotted together for a global linear regression. The fitting was forced to pass through the zero point, and the yielded slope is 1.02±0.03 (r^2=0.95). Error bars were assumed 10% relative (note that the uncertainty of our data was usually <10% and mostly <5% relative: see text)

This is a preprint, the final version is subject to change, of the American Mineralogist (MSA)
Cite as Authors (Year) Title. American Mineralogist, in press.
DOI: https://doi.org/10.2138/am-2018-6620

580 Table 1 Summary of olivine, clinopyroxene and orthopyroxene samples and H_2O contents

No.[a]	ppm H_2O (polarized)[b]		ppm H_2O (unpolarized, Method 1)[c]			ppm H_2O (unpolarized, Method 2)[d]			summary of samples[e]			
	(reported)	(reprocessed)	(plane 1)	(plane 2)	(mean)	(plane 1)	(plane 2)	(mean)	*P* (GPa)	*T* (ºC)	fO_2 *buffer*	Reference
oli(PC11)	240	237	68	91	79.5	230	310	270	3.5	1100	NNO	Yang et al. (2014b)
oli(1)	90	97	29	30	29.5	82	86	84	1	1100	IW	Yang (2015)
oli(4)	43	38	16	16	16	32	67	49	1	1100	IW	Yang (2015)
oli(6)	195	184	100	37	68.5	248	155	201	3	1100	IW	Yang (2015)
oli(15)	175	165	46	76	61	153	231	192	3	1100	IW	Yang (2015)
oli(5)	200	212	77	51	64	233	173	203	3	1100	IW	Yang (2015)
oli(11)	200	190	64	52	58	191	130	161	2.5	1100	NNO	Yang (2016)
oli(12)	254	262	55	56	55.5	233	217	225	2.5	1100	HM	Yang (2016)
oli(9)	138	127	26	25	25.5	88	74	81	1.5	1300	NNO	Yang (2016)
oli(18)	400	422	175	157	166	561	454	508	5	1100	NNO	Yang (2016)
oli(oli-0)	436	423	133	154	143.5	404	449	426	7	1100	NNO	Shuai and Yang (2017)
oli(oli-1)	23	26	9	7	8	33	30	31	1	900	NNO	Shuai and Yang (2017)
oli(oli-3)	70	75	28	23	25.5	94	76	85	2.5	1200	NNO	Shuai and Yang (2017)
oli(oli-6)	61	66	12	44	28	58	58	58	1	1100	NNO	Shuai and Yang (2017)
cpx(natural)		48	19	20	20	38	41	39	-	-	-	this study
cpx(A67)		279	140	207	174	235	278	257	3	1100	IW	this study
cpx(A69)		146	156	103	129	186	148	167	2	1100	HM	this study
opx(natural)		31	25	21	23	36	29	33	-	-	-	this study
opx(A85)		173	104	144	124	119	141	130	2	1100	IW	this study
opx(A60)		65	69	38	54	88	47	67	1	1000	NNO	this study

581 [a] Labels in the parentheses are the sample as used in the referred literatures.

582 [b] Values labeled as ‘reported’ are taken from the referred literatures directly, and values labeled as ‘reprocessed’ are the recalculated data from

583 the re-measured FTIR spectra of this study. The slight differences are caused by the arbitrary uncertainty due to performing baseline
584 corrections by different operators, but are generally within 10% relatively (mostly <5%). All the data are calculated from three polarized FTIR
585 spectra along three mutually perpendicular directions of each sample crystal (see text for more details). oli samples are from the same starting
586 crystal from Dak Lak, Vietnam, cpx samples are from the same starting crystal from Asku, China, and opx samples are from the same starting
587 crystal from Tanzania (see text for details).

588 [c] Values for the spectra taken along two perpendicular planes by the unpolarized Method 1 and the average data (see text for details).

589 [d] Values for the spectra taken along two perpendicular planes by the unpolarized Method 2 and the average data (see text for details).

590 [d] Abbreviations of fO_2 buffers: NNO, Ni-NiO; IW, Fe-FeO; HM, Fe_2O_3-Fe_3O_4.

591 Uncertainty of H_2O contents is usually <10% relative (see text).

592

This is a preprint, the final version is subject to change, of the American Mineralogist (MSA)
Cite as Authors (Year) Title. American Mineralogist, in press.
DOI: https://doi.org/10.2138/am-2018-6620

593 Table 2 H_2O contents of clinopyroxene and orthopyroxene samples by unpolarized
594 analyses on 10 randomly oriented grains

No.	ppm H_2O[a]										
	(randomly oriented grains)										(mean)
Cpx(*natural*)	48*										
unpolarizd, Method 1	14	24	21	29	36	22	36	34	22	25	26
unpolarizd, Method 2	28	50	47	58	75	36	76	72	30	35	51
Opx(*natural*)	31*										
unpolarizd, Method 1	23	25	21	21	15	18	18	21	21	26	21
unpolarizd, Method 2	34	34	30	29	18	24	27	26	33	41	30

595 [a] Values for the unpolarized spectra taken from randomly oriented grains and the average
596 data.

597 * H_2O contents by polarized analyses are shown for reference (the values are also given
598 in Table 1).

599 Uncertainty of H_2O contents is usually <10% relative (see text).

600

This is a preprint, the final version is subject to change, of the American Mineralogist (MSA)
Cite as Authors (Year) Title. American Mineralogist, in press.
DOI: https://doi.org/10.2138/am-2018-6620

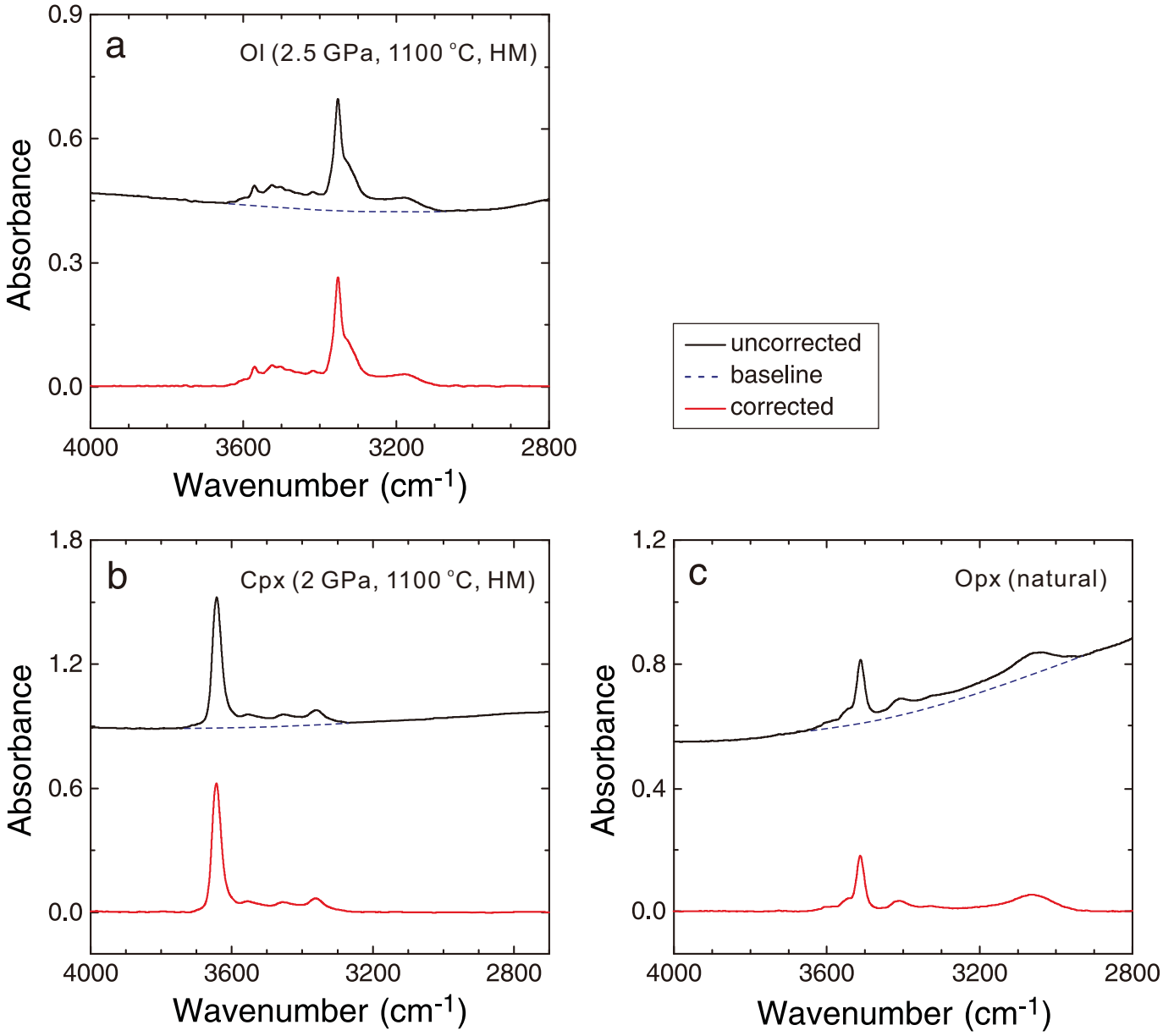

Fig. 1

This is a preprint, the final version is subject to change, of the American Mineralogist (MSA)
Cite as Authors (Year) Title. American Mineralogist, in press.
DOI: https://doi.org/10.2138/am-2018-6620

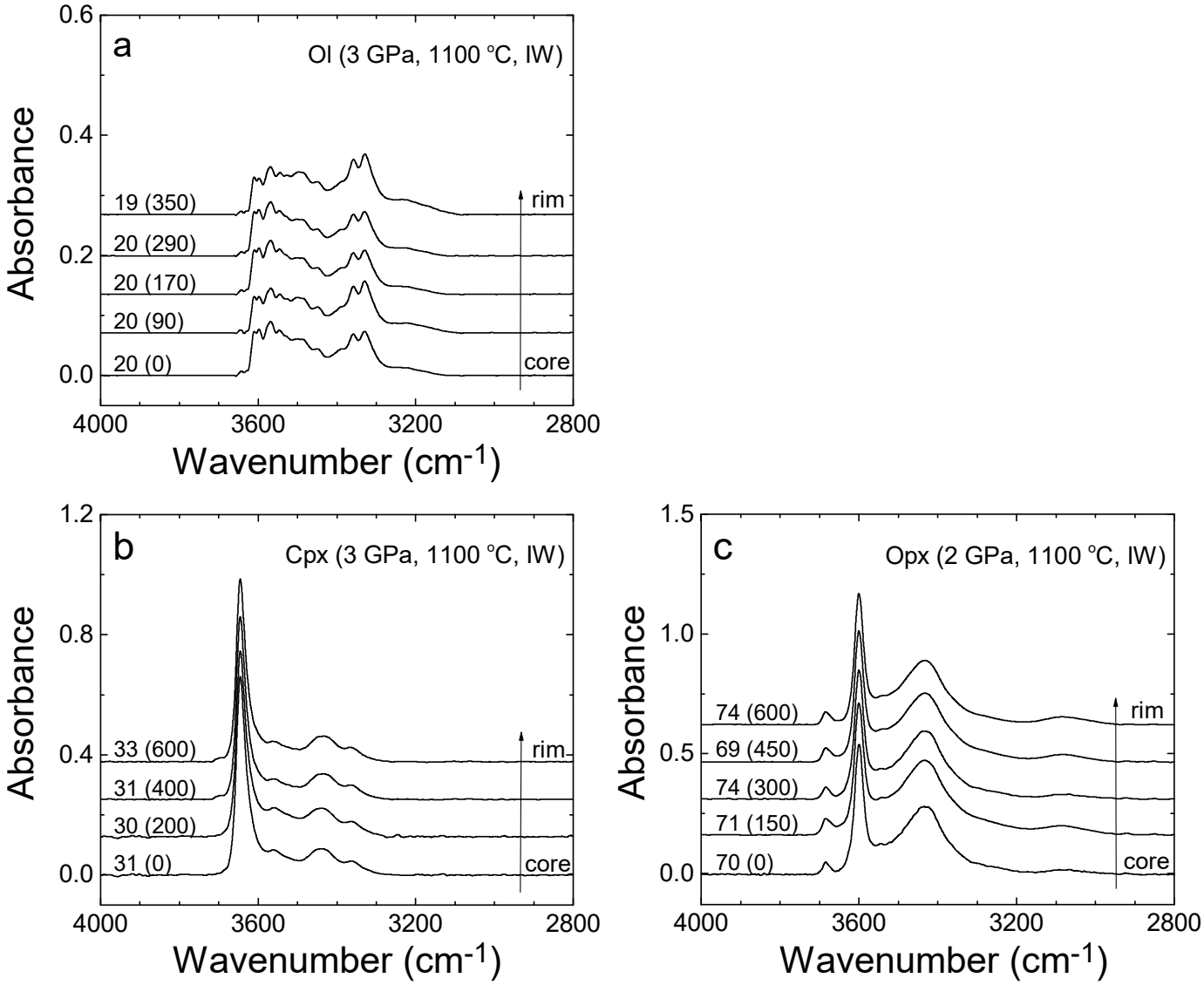

Fig. 2

This is a preprint, the final version is subject to change, of the American Mineralogist (MSA)
Cite as Authors (Year) Title. American Mineralogist, in press.
DOI: https://doi.org/10.2138/am-2018-6620

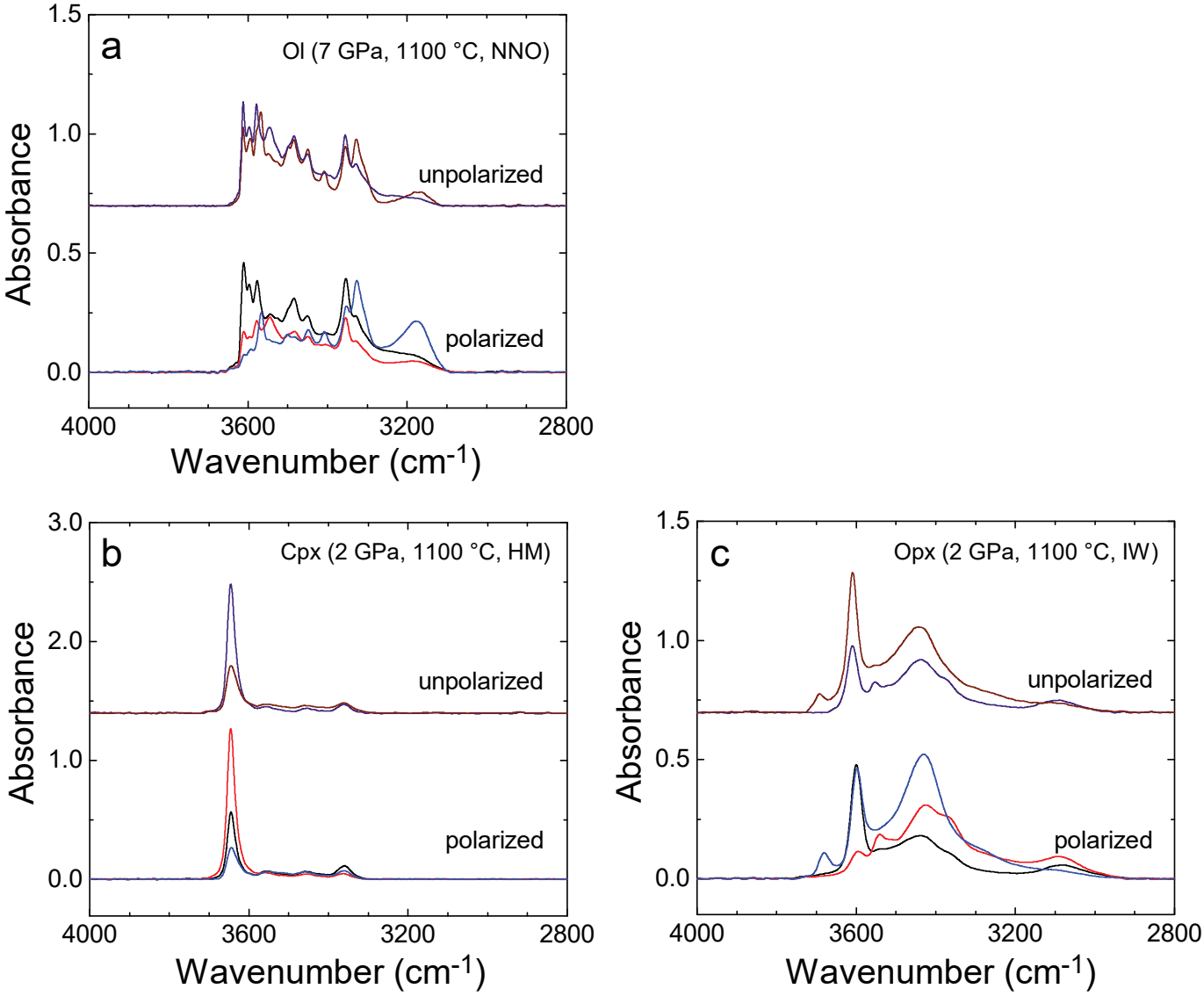

Fig. 3

This is a preprint, the final version is subject to change, of the American Mineralogist (MSA)
Cite as Authors (Year) Title. American Mineralogist, in press.
DOI: https://doi.org/10.2138/am-2018-6620

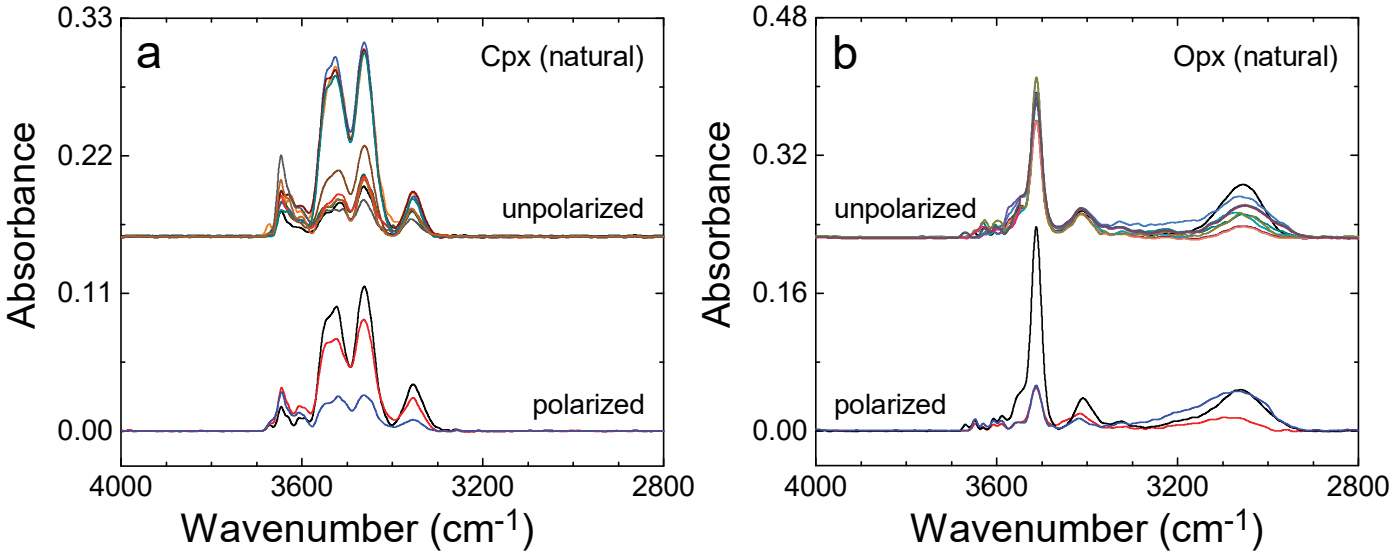

Fig. 4

This is a preprint, the final version is subject to change, of the American Mineralogist (MSA)
Cite as Authors (Year) Title. American Mineralogist, in press.
DOI: https://doi.org/10.2138/am-2018-6620

Open symbols, single grain; Solid symbols, mean value

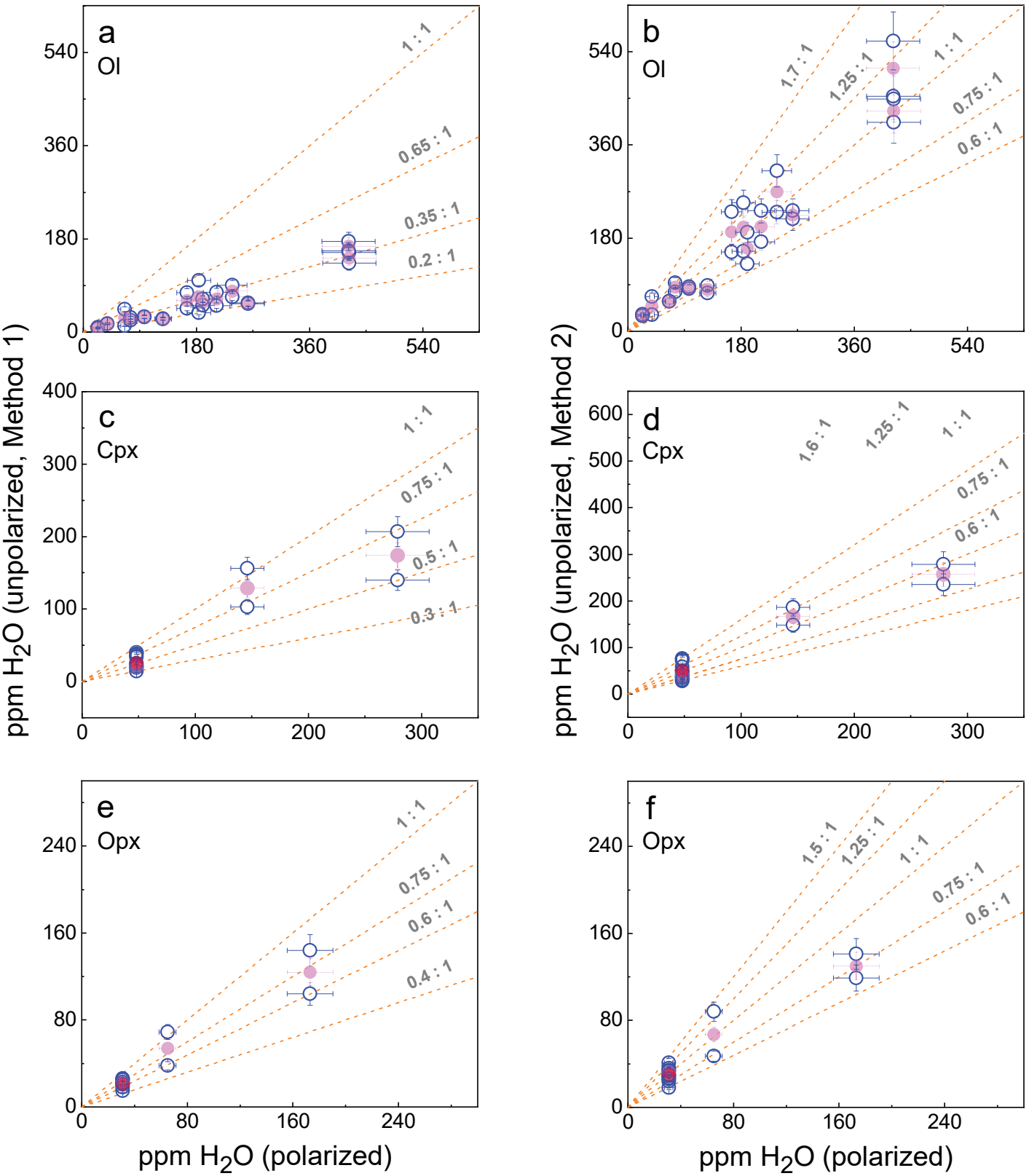

Fig. 5

This is a preprint, the final version is subject to change, of the American Mineralogist (MSA)
Cite as Authors (Year) Title. American Mineralogist, in press.
DOI: https://doi.org/10.2138/am-2018-6620

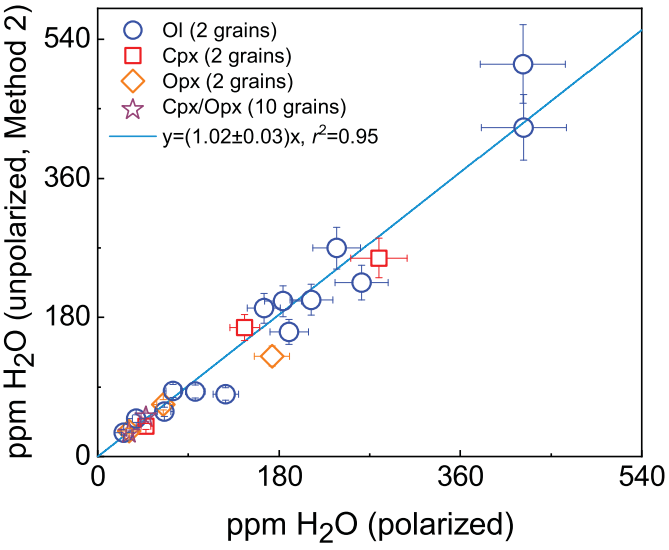

Fig. 6